Sensitivity analysis of source region size on results of Stochastic Noise Generation and Radiation model

Pavel NIEDOBA[1]; Jaroslav BAJKO[1]; Miroslav JÍCHA[1]; Libor ČERMÁK[1]

[1] Brno University of Technology, Czech Republic

ABSTRACT

The paper deals with the Stochastic Noise Generation and Radiation (SNGR) model based on synthesizing of turbulent velocity components from results of a Reynolds Averaged Navier-Stokes (RANS) simulation. The turbulent velocity components are then used for computation of aero-acoustic sources representing the right-hand side of linerized Euler equations (LEE) describing the sound propagation. Primarily, the paper is aimed on testing the sensitivity of SNGR model solution on a source region size. Specifically, an acoustic intensity was chosen as a comparative variable computed by solving LEE via meshfree Finite Point Method (FPM). The size of source region has a direct impact on time and memory requirements during the stochastic reconstruction. As a test case, we chose a 2D free plane jet with height $2b_0 = 30\,\mathrm{mm}$ and $M = 0.1$. For obtaining the averaged flow results, the RANS simulation with standard $k-\varepsilon$ turbulence model was performed. Based on this averaged results, the turbulent velocity field is obtained by the synthesis of a finite sum of random Fourier modes.

Keywords: Stochastic Noise Generation and Radiation model, Aero-acoustic source term, Jet noise

1. INTRODUCTION

Aero-acoustics (AA) is interdisciplinary science that deals with flow-induced sound. This branch of acoustics began about 60 years ago, mainly caused by the invention of jet planes and efforts to reduce their noise levels. For many practical challenges to reduce noise in industrial applications, the ability to predict and understand generation of noise is very important. The recent renewed interest in AA is due to increasing computing resources.

Computational Aero-Acoustics (CAA) is a tool for numerical simulation of sound. The CAA can be divided into two approaches. The first approach consists of direct methods where the full compressible Navier-Stokes equations are solved using Large Eddy Simulation (LES) or Direct Numerical Simulation (DNS). Unfortunetally, this first approach is still unusable for most practical applications due to the enormous computational demands. The time inconveniences caused by direct methods are at least partially overcome by the second approach, the hybrid methods. These methods are often referred to as two-step methods on grounds of a division of problem on a sound generation part, and a sound propagation part. If we focus on the generation of sound, the turbulent velocity field is necessary for acoustic source term computation. One way to obtain these turbulent fluctuations may be performing the unsteady simulation, e.g. DNS, or LES. The second way can be the stochastic reconstruction of turbulent velocity field from the low cost RANS simulation, e.g. closed with a $k-\varepsilon$ turbulence model, where k is the turbulent kinetic energy and ε is the turbulence dissipation rate. This stochastic reconstruction is used in SNGR model where the turbulent velocity field is synthesized by a finite sum of random Fourier modes. Now, if we focus on the propagation of sound, we use LEE with the source term on the right hand side which is calculated using the turbulent velocity field.

The SNGR model is based on the approach devised by Kraichnan (1) and improved by Karweit *et al.* (2), where the spatially correlated turbulent velocity field is defined as a finite sum of discrete Fourier modes. This method was originally used for generating a turbulent velocity field from the turbulent quantities obtained by RANS simulation, and subsequent computing of acoustic source terms as a right hand side of appropriate propagation equations of sound waves. The first formulation of this model was applied to subsonic jet noise calculation by Béchara *et al.* (3). In a further development, Bailly *et al.* (4) introduced a time dependent term into the Fourier modes. A different way of introducing time dependency based on an asymmetric time filter was presented by Billson *et al.* (5).

[1]niedoba@fme.vutbr.cz

2. STOCHASTIC NOISE GENERATION AND RADIATION MODEL

2.1 Stochastic turbulence modeling

The method for generating a homogeneous isotropic turbulence having the proper spatial characteristics was proposed in (1). The turbulent velocity field is defined using the Fourier mode approach.

Consider a Fourier decomposition of a turbulent homogeneous isotropic field $\mathbf{u}' = (u'_1, u'_2, u'_3)$ at given point $\mathbf{x} = (x, y, z)$

$$\mathbf{u}'(\mathbf{x}) = \int \hat{\mathbf{u}}(\boldsymbol{\kappa}) e^{j\boldsymbol{\kappa}\cdot\mathbf{x}} \mathrm{d}\boldsymbol{\kappa} \tag{1}$$

where $\boldsymbol{\kappa}$ is a wave vector and j is the unit imaginary number ($j^2 = -1$). Assuming that $\mathbf{u}'$ is a real function, and using the even property of cosine function, we may approximate the equation 1 as a finite sum of N discrete Fourier modes

$$\mathbf{u}'(\mathbf{x}) = 2 \sum_{n=1}^{N} \hat{u}^n \cos(\boldsymbol{\kappa}^n \cdot \mathbf{x} + \psi^n) \boldsymbol{\sigma}^n \tag{2}$$

where $\hat{u}^n$, ψ^n, and $\boldsymbol{\sigma}^n$ are the amplitude, phase, and direction, respectively, of the nth Fourier mode associated with the wave vector $\boldsymbol{\kappa}^n$. Each wave vector $\boldsymbol{\kappa}^n$ is picked randomly on a sphere of radius specified by a wave number $\kappa^n = ||\boldsymbol{\kappa}^n||$ to ensure isotropy. Hence, the wave vector κ^n may be characterized by spherical coordinates $(\kappa^n, \varphi^n, \theta^n)$.

Now we define the choice of wave numbers κ^n. The highest wave number is dependent on a mesh resolution, i.e. $\kappa_{max} = \pi/\Delta$, where Δ is equal to grid spacing, when we have an equidistant grid. In the case of non-equidistant grid, we may decide to pick a mean value of grid spacing as a Δ. The smallest wave number is defined by relation $\kappa_{min} = \kappa_e/p$, where $\kappa_e = A9\pi/(55L_t)$ is the wave number corresponding to the most energy containing eddies (6), p is the parameter which should be larger then one to make the smallest wave number smaller then κ_e. The numerical constant A will be introduced later, and $L_t = (2k/3)^{3/2}/\varepsilon$ is a turbulent length scale. Now, we may divide the wave number range, from κ_{min} to κ_{max}, into N equally large segments of size $\Delta\kappa$. The center of nth segment then corresponds to the nth wave number κ^n.

We also assume an incompressibility of the turbulent field and hence, the relation

$$\boldsymbol{\kappa}^n \cdot \boldsymbol{\sigma}^n = 0, \qquad n = 1, \ldots, N \tag{3}$$

is satisfied (3). Therefore in a spectral space, the unit vector $\boldsymbol{\sigma}^n$ is always perpendicular to the wave vector $\boldsymbol{\kappa}^n$, and its direction on the plane perpendicular to $\boldsymbol{\kappa}^n$ is determined by the polar angle α^n. As a consequence of isotropy, homogeneity, and incompressibility, the angles $\varphi^n, \theta^n, \alpha^n$ and ψ^n are chosen randomly with probability distributions given in table 1 (7).

Table 1 – Probability distributions of the random angles

$p(\varphi^n) = 1/(2\pi)$	$0 \le \varphi^n \le 2\pi$
$p(\theta^n) = (1/2)\sin\theta^n$	$0 \le \theta^n \le \pi$
$p(\alpha^n) = 1/(2\pi)$	$0 \le \alpha^n \le 2\pi$
$p(\psi^n) = 1/(2\pi)$	$0 \le \psi^n \le 2\pi$

For a complete description of the turbulent velocity field $\mathbf{u}'(\mathbf{x})$, see equation 2, we have to determine the amplitude $\hat{u}^n$ of nth Fourier mode. A relation between k and $\hat{u}^n$ should be established using the equation 2 as in (3).

$$k = \sum_{n=1}^{N} (\hat{u}^n)^2 \tag{4}$$

For the homogeneous isotropic turbulence, the energy spectrum $E(\kappa)$ satisfies the following equality (8)

$$\int_0^\infty E(\kappa) \mathrm{d}\kappa = k \tag{5}$$

Now its clear, from the relations 4 and 5, that our approximation given by equation 2 allow us to approximate the integral of energy spectrum by the finite sum of squares of Fourier mode amplitudes. Hence, the amplitude of nth Fourier mode is given by

$$\hat{u}^n = \sqrt{E(\kappa^n)\Delta\kappa} \tag{6}$$

The modified Von Kármán spectrum is employed to simulate the isotropic energy spectrum (3)

$$E(\kappa) = A\frac{u'^2_{rms}}{\kappa_e}\frac{(\kappa/\kappa_e)^4}{[1+(\kappa/\kappa_e)^2]^{17/6}}\exp[-2(\kappa/\kappa_\eta)^2] \tag{7}$$

where $\kappa_\eta = \varepsilon^{1/4}\nu^{-3/4}$ is the Kolmogorov wave number, $u'_{rms} = \sqrt{2k/3}$ is a root mean square value of the turbulent velocity field $\mathbf{u}'$, and A is the earlier mentioned numerical constant set to fulfill the relation 5. Thus (7),

$$A = \frac{55}{9\sqrt{\pi}}\frac{\Gamma(5/6)}{\Gamma(1/3)} \tag{8}$$

For completeness, we should note that the symbol ν denotes a kinematic viscosity.

Now, we define a time sequence $\{\mathbf{u}'(\mathbf{x},t)\}_{t=0}^{T}$ of the random turbulent velocity field $\mathbf{u}'(\mathbf{x})$ (see equation 2), where T is a total time. This time sequence corresponds to the generation of fluctuations at each time step. Until the individual members $\mathbf{u}'(\mathbf{x},t)$ of the sequence are independent of each other, the time correlation will be zero, which is unphysical.

To introduce a time dependency, we adopt the approach proposed in (5), where the field at current time step is computed as a weighted sum of the field at previous step, and the random field generated by relation 2. Thus, the time correlated random turbulent velocity field $\mathbf{v}' = (v'_1, v'_2, v'_3)$ is obtained as follows

$$\begin{aligned} \mathbf{v}'(\mathbf{x},t) &= a\mathbf{v}'(\mathbf{x},t-\Delta t) + b\mathbf{u}'(\mathbf{x},t) \qquad && t = \Delta t,\dots,T \\ \mathbf{v}'(\mathbf{x},t) &= \mathbf{u}'(\mathbf{x},t) && t = 0, \end{aligned} \tag{9}$$

where Δt denotes a time step, $a = \exp(-\Delta t/T_t)$ is the weighting coefficient, by which the turbulent time scale $T_t = k/\varepsilon$ is prescribed (5), and the choice of the coefficient $b = \sqrt{1-a^2}$ ensures a preservation of the root mean square values of the random turbulent velocity fields (6), i.e. $v'_{rms} = u'_{rms}$.

2.2 Linearized Euler equations

Let us denote the vector function $\mathbf{w}(\mathbf{x},t) := (\rho(\mathbf{x},t), v_1(\mathbf{x},t), v_2(\mathbf{x},t), p(\mathbf{x},t))^T$ with primitive (physical) variables, i.e. the density, velocity components and pressure, respectively. Therefore, the compressible 2D Euler equations in matrix form read as

$$\frac{\partial \mathbf{w}}{\partial t} + \mathbb{A}_1(\mathbf{w})\frac{\partial \mathbf{w}}{\partial x} + \mathbb{A}_2(\mathbf{w})\frac{\partial \mathbf{w}}{\partial y} = \mathbf{0}, \quad \mathbf{x} = (x,y) \in \mathbb{R}^2,\, t > 0, \tag{10}$$

where the Jacobian matrices of this hyperbolic system are given as follows

$$\mathbb{A}_1(\mathbf{w}) = \begin{pmatrix} v_1 & \rho & 0 & 0 \\ 0 & v_1 & 0 & 1/\rho \\ 0 & 0 & v_1 & 0 \\ 0 & \gamma p & 0 & v_1 \end{pmatrix}, \quad \mathbb{A}_2(\mathbf{w}) = \begin{pmatrix} v_2 & 0 & \rho & 0 \\ 0 & v_2 & 0 & 0 \\ 0 & 0 & v_2 & 1/\rho \\ 0 & 0 & \gamma p & v_2 \end{pmatrix}, \tag{11}$$

where γ is the adiabatic index ($\gamma = 1.4$ for diatomic gases). The quantities included in $\mathbf{w}$ can be decomposed into a *reference state* (or *mean value*) $\mathbf{w}_0(\mathbf{x})$ and a time dependent *acoustic fluctuating* (or *perturbation*) part $\mathbf{w}'(\mathbf{x},t)$, cf. (9, 10, 11) in the following way

$$\mathbf{w} = \begin{pmatrix} \rho \\ v_1 \\ v_2 \\ p \end{pmatrix} = \underbrace{\begin{pmatrix} \rho_0 \\ v_{1,0} \\ v_{2,0} \\ p_0 \end{pmatrix}}_{\mathbf{w}_0} + \underbrace{\begin{pmatrix} \rho'_{ac} \\ v'_{1,ac} \\ v'_{2,ac} \\ p'_{ac} \end{pmatrix}}_{\mathbf{w}'}, \quad \mathbf{x} = (x,y) \in \mathbb{R}^2, t > 0. \tag{12}$$

Assuming that the fluctuating variables $\mathbf{w}'$ are negligible in comparison to the reference states $\mathbf{w}_0$, i.e.

$$|\rho'_{ac}| \ll |\rho_0|,\ |v'_{1,ac}| \ll \|\mathbf{v}_0\|,\ |v'_{2,ac}| \ll \|\mathbf{v}_0\|,\ |p'_{ac}| \ll |p_0|, \tag{13}$$

where $\mathbf{v}_0 = (v_{1,0}, v_{2,0})^T$, the Jacobian matrices $\mathbb{A}_i(\mathbf{w})$ can be approximated as follows

$$\mathbb{A}_i(\mathbf{w}_0 + \mathbf{w}') \approx \mathbb{A}_i(\mathbf{w}_0), \qquad i = 1,2. \tag{14}$$

Substituting $\mathbf{w} = \mathbf{w}_0 + \mathbf{w}'$ into equation 10 and arranging the equations with respect to the unknown fluctuating variables $\mathbf{w}'$, the 2D linearized Euler equations in matrix form read as

$$\frac{\partial \mathbf{w}'}{\partial t} + \mathbb{A}_1(\mathbf{w}_0)\frac{\partial \mathbf{w}'}{\partial x} + \mathbb{A}_2(\mathbf{w}_0)\frac{\partial \mathbf{w}'}{\partial y} = \mathbf{S}, \tag{15}$$

where $\mathbb{A}_1(\mathbf{w}_0)$, $\mathbb{A}_2(\mathbf{w}_0)$ are linearized Jacobian matrices and $\mathbf{S}$ is the source term.

2.3 Aero-acoustic source terms

Aero-acoustic source terms represent an intermediate step of CAA hybrid methods. The calculation of these source terms is based on known mean and turbulent velocity fields. In our case, the turbulent velocity field is obtained by the stochastic reconstruction using turbulent results of RANS simulation, ie. turbulent kinetic energy and turbulence dissipation rate. The acoustic analogy asociated with LEE has been developed in order to solve the propagation of acoustic waves in non-uniform mean flow (4). Similarly as in (11), we choose the acoustic source term in following form

$$\mathbf{S} = (\ 0,\ S_1,\ S_2,\ 0\ )^T, \tag{16}$$

where

$$S_i = -\frac{\partial \rho_0\, v'_i v'_j}{\partial x_j} + \overline{\frac{\partial \rho_0\, v'_i v'_j}{\partial x_j}}, \qquad i = 1,2. \tag{17}$$

3. RESULTS

3.1 Flow results

As a test case, we chose a 2D free plane jet with height $2b_0 = 30\,\text{mm}$ and inlet velocity $U_0 = 34.7\,\text{ms}^{-1}$ corresponding to Mach number $M = 0.1$. Kinematic viscosity $\nu = 15.29 \cdot 10^{-6}\,\text{m}^2\text{s}^{-1}$ is set for air at the temperature $\tau = 20°\text{C}$. From resulting Reynolds number $Re = 68{,}084$, we can assume that flow is fully turbulent. We use the same domain configuration, boundary conditions, and mesh settings as Aloysius (12). This case was experimentaly investigated by Forthmann (13) and well described also by Abramovich (14) where the theoretical solution of axial velocity progress was derived.

We use these data for proper setting of turbulent kinetic energy k at the inlet, because there is not any inlet turbulence information in the Forthmann's experiment. Hence, we performed a precursor pipe flow simulation to obtain at least estimation of turbulent kinetic energy and turbulence dissipation rate inlet profiles. Figure 1 shows good agreement of axial velocity $v_{1,0}$ with the experimental and theoretical data. Constant $a = 0.11$, see Figure 1, provides the best fit to Forthmann's experiment (12). For the purpose of generation of stochastic turbulent velocity field, see equation 2, we perform RANS simulation with $k - \varepsilon$ closure providing required inputs, ie. turbulent kinetic energy k and turbulence dissipation rate ε. Figure 2 illustrates the mean axial velocity component of our case.

For the purpose of stochastic reconstruction (see section 2.1), we set the number of Fourier modes $N = 100$ and parametr $p = 5$ (7). Once the turbulent velocity field is generated (see equation 2), the acoustic source term may be computed according to equation 17. Note that this source term represent the right-hand side of the 2D linearized Euler equations (see equation 15).

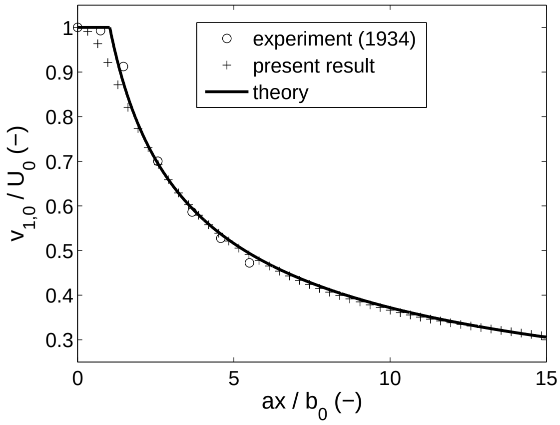

Figure 1 – Axial velocity decay along the axis of the jet

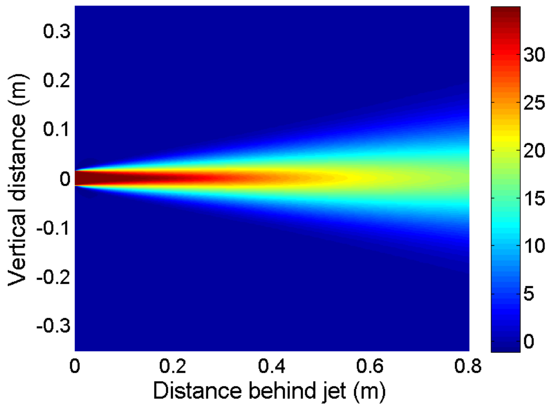

Figure 2 – Mean axial velocity (ms^{-1})

3.2 Acoustic results

Solution of LEE (see equation 15) representing the sound propagation is based on meshfree Finite Point Method (FPM) described by Bajko (15). The computation was carried out on an acoustic mesh that consists of 11,684 mesh points with local refinement near the jet exit (see Figure 3). The sides adjacent to the jet exit are set up as walls. The other boundaries represent a free space, where a sponge layer is estabilished. The sponge layer is used for absorption of sound waves and thus it prevents them from the returning back to the domain. The time step $\Delta t = 10^{-6}$ s. The computation covers a time interval $T = 10^{-2}$ s, which corresponds to 10,000 time steps. The acoustic pressure is computed at locations on the part of circle with diameter $R = 39b_0$ centered at the jet exit and emission angles $\theta \in \{5°, 10°, \ldots, 85°\}$ (see Figure 4).

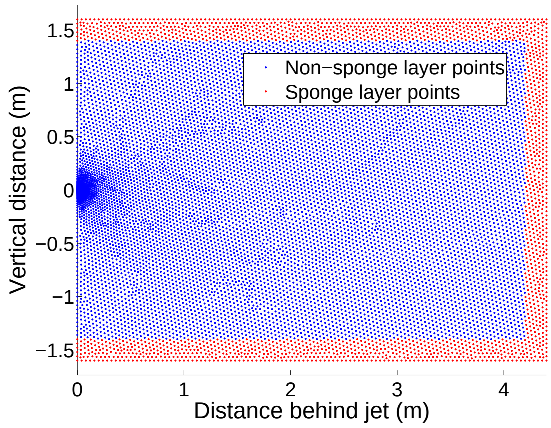

Figure 3 – Acoustic mesh with sponge layer

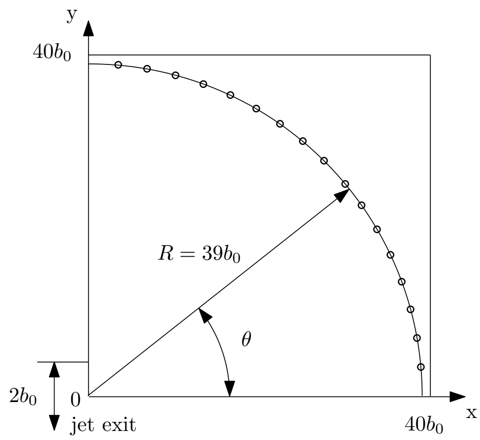

Figure 4 – Location of probes ○

The evaluation of acoustic intensity is performed over the last 5,000 time steps of computation. The first 5,000 time steps represent the transition to steady-state regime and hence they are not considered.

For comparative purposes, we define the acoustic intensity, ie.

$$L_I = 10 \log \left(\frac{I}{I_{ref}} \right), \tag{18}$$

where $I_{ref} = 10^{-12}\,\mathrm{Wm}^{-2}$ and

$$I = \overline{p'_{ac} \cdot \sqrt{{v'_{1,ac}}^2 + {v'_{2,ac}}^2}}\,. \tag{19}$$

Furthermore, we introduce the size of source region which is limited to points where the turbulent kinetic energy, cf. Mesbah *et al.* (16)

$$k > A_c k_{max}\,, \tag{20}$$

where k_{max} is the maximum value of k, and cut coefficient $A_c \in <0,1>$ determines the size of source region by neglecting the points with turbulent kinetic energy less than $A_c k_{max}$ and at these points, we set the source term (see equation 17) equal to zero, ie.

$$\mathbf{S} = \mathbf{0}\big|_{k \leq A_c k_{max}}. \tag{21}$$

Note, for example, $A_c = 0.1$ (or 10%) means that the points with kinetic energy less than $0.1k_{max}$ are not taken into account, ie. these points do not contribute to the source region. The figure 5 shows the dependencies of acoustic intensity L_I on emission angle θ for different values of cut coefficient A_c. We may see that the acoustic intensity decreases with the increasing emission angle. If we assume that the solution for $A_c = 0$ is the correct solution, we can notice that the accuracy decreases with an increase of cut coefficient A_c. In the figure 6, the acoustic pressure p'_{ac} is shown at time $t = 0.01$ s.

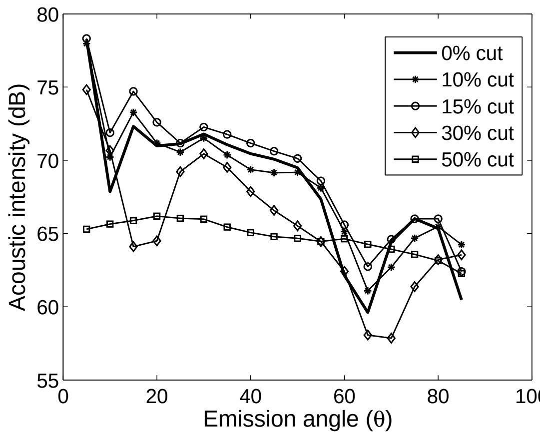

Figure 5 – Acoustic intensity at different emission angles θ

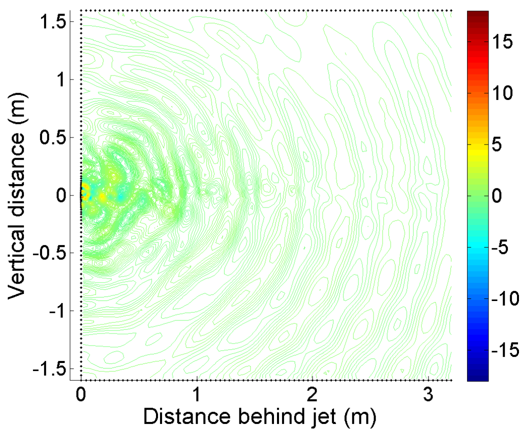

Figure 6 – Acoustic pressure (Pa), $A_c = 0$

Figure 7 shows the accuracy deviation δ defined in the following way

$$\delta(A_c) = \sum_{\theta} \frac{|L_I(\theta) - L_I^{A_c}(\theta)|}{L_I(\theta)}, \tag{22}$$

where $L_I^{A_c}$ is the acoustic intensity for specific value of cut coefficient A_c. Note that $L_I = L_I^0$. From this figure, we are able to determine which values of cut coefficient A_c are still acceptable. The values of $A_c \leq 20\%$ seem to be a suitable choice for this case (the error is less than 5%). Moreover, the value of A_c has a direct impact on computational demands when the stochastic turbulent velocity field is generated. The computation is limited only to the points satisfying the relation 20. The memory requirements and time costs decrease significantly with increasing of cut coefficient A_c (see Figure 8) during the stochastic reconstruction.

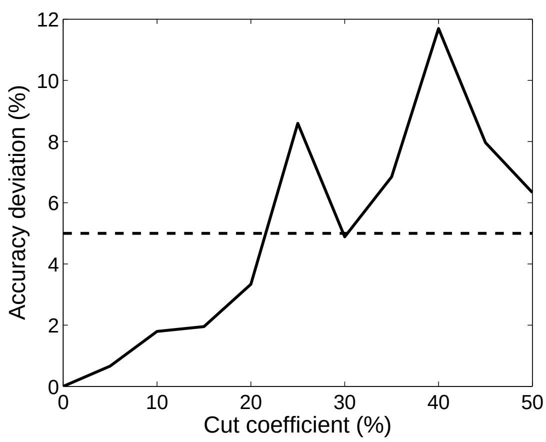

Figure 7 – Accuracy deviation; - - - : 5% error

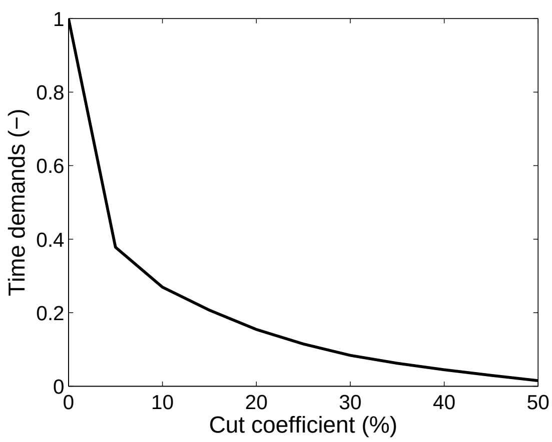

Figure 8 – Normalized time cost of one time step

4. CONCLUSION

This paper describes the Stochastic Noise Generation and Radiation (SNGR) model and its application to low Mach number free jet application.

We mainly tested the influence of source region size on the SNGR model solution, specifically an acoustic intensity was chosen as a comparative variable. The size of source region is determined by a cut coefficient which specifies the points contributing to source region based on the value of turbulent kinetic energy. It can be seen that this cut coefficient has direct impact on accuracy and time demands of calculation. Hence, we try to set the largest possible value of this cut coefficient fulfilling the required accuracy. Note that the increasing cut coefficient significantly decreases the time costs of the stochastic reconstruction and hence of the entire SNGR model.

ACKNOWLEDGMENTS

This research was supported by the Czech Grant Agency under the grant GA 13-27505S.

REFERENCES

1. Kraichnan RH. Diffusion by a random velocity field. Physics of Fluids. 1970;13(1):22–31.

2. Karweit M, Blanc-Benon P, Juve D, Comte-Bellot G. Simulation of the propagation of an acoustic wave through a turbulent velocity field: A study of phase variance. J Acoust Soc Am. 1991;89(1):52–62.

3. Béchara W, Bailly C, Lafon P, Candel SM. Stochastic Approach to Noise Modeling for Free Turbulent Flows. AIAA Journal. 1994;32(3):455–463.

4. Bailly C, Lafon P, Candel S. A Stochastic Approach to Compute Noise Generation and Radiation of Free Turbulent Flows. AIAA paper. 1995;95-092(1):669–674.

5. Billson M, Eriksson LE, Davidson L. Jet Noise Prediction Using Stochastic Turbulence modeling. AIAA paper. 2003;2003-3282(1):1–3.

6. Davidson L. Using isotropic synthetic fluctuations as inlet boundary conditions for unsteady simulations. Advances and Applications in Fluid Mechanics. 2007;1:1–35.

7. Bailly C, Juvé D. A Stochastic Approach To Compute Subsonic Noise Using Linearized Eulers's Equations. AIAA paper. 1999;99-1872(1):496–506.

8. Hinze JO. Turbulence. New York: McGraw-Hill; 1975.

9. Roeck WD. Hybrid Methodologies for the computational Aeroacoustic Analysis of Confined, Subsonic Flows. Katholieke Universiteit Leuven; 2007. PhD thesis.

10. Ali I, Becker S, Utzmann J, Munz CD. Aeroacoustic study of a forward facing step using linearized euler equations. Physica D. 1999;237(1):2184–2189.

11. Bailly C, Juvé D. Numerical solution of acoustic propagation problems using linearized euler equations. AIAA Journal. 2000;38(1):22–29.

12. Aloysius SS, Wrobel LC. Comparison of flow and dispersion properties of free and wall turbulent jets for source dynamics characterisation. Environ Modelling & Software. 2009;24:926–937.

13. Forthmann E. Turbulent Jet Expansion. NACA Technical Memorandum. 1936;TM-789. English Translation.

14. Abramovich GN. The Theory of Turbulent Jets. Cambridge, Massachuse: The M.I.T. Press; 1963.

15. Bajko J, Čermák L, Jícha M. High order finite point method for the solution to the sound propagation problems. Comput Methods in Appl Mech and Engrg. 2014;280:157–175.

16. Mesbah M, Meyers J, Baelmans M, Desmet W. Assessment of Different Parameters Used in the SNGR Method. Proceedings of ISMA2004. 2004;p. 389–402.